Relay Selection for Cognitive Massive MIMO Two-Way Relay Networks

Shashindra Silva, Masoud Ardakani and Chintha Tellambura
Department of Electrical and Computer Engineering, University of Alberta, Edmonton, AB, Canada T6G 2V4
Email: {jayamuni, ardakani, chintha}@ualberta.ca

***Abstract*—We analyze relay selection for an underlay cognitive radio (CR) two-way relay network (TWRN) with zero-forcing (ZF) transmission and receiving. The source and the destination nodes are massive multiple-input multiple-output (MIMO) enabled. Relays will perform amplify and forwarding (AF) while the destination and source nodes perform self interference cancellation. We first obtain asymptotic signal-to-interference-plus-noise ratio (SINR) values under the power scaling at the relay and end nodes. Then, we derive optimal power allocation schemes for the end nodes to satisfy the interference constraints at the primary user (PU). Based on these optimal values, we analyze the effect of relay selection on the sum rate. With the use of massive MIMO, the SINR and the sum rate will only depend on the pathloss coefficients of the channels and average noise levels. Thus, the relay selection can be done at the deployment stages of the system and most of the time it simplifies to selection of the relay with the highest number of antennas. Our simulation results validate the analytical asymptotic results and qualify CR massive MIMO TWRNs as a possible candidate for future wireless systems.**

I. Introduction

Global mobile traffic data increased by 74% in year 2015 and will increase by eightfold during the next five years [1]. This exponential increase in demand for wireless data has resulted in spectrum scarcity in current wireless systems. Thus, effective reuse of the wireless spectrum is important for wireless systems. Cognitive radio (CR) has been proposed as an efficient spectrum reuse and sharing technology for wireless systems [2]. Underlay CR allows secondary users to use the same bandwidth of primary users (PUs) without exceeding a certain interference threshold at the PUs [3].

Two-way relay networks (TWRNs) enable bi-directional data transmission between two nodes via a relay node [4]. TWRNs double the spectral efficiency compared to a one-way relay and are currently being used for several wireless communication standards, including Longterm evolution-advanced (LTE-A) [5]. Use of multiple-input multiple-output (MIMO) technology in TWRNs further improves the achievable data rate and the reliability of TWRNs due to the spatial multiplexing and diversity gains [6], [7]. Massive MIMO is the extension of MIMO systems by using a very large antenna array at the end nodes [8]. Massive MIMO mitigates the effects of small-scale fading and interferences due to the improved degrees of freedom offered by large antenna arrays [9]. Also, it offers optimal linear beamforming and precoding methods and increased power efficiencies. Henceforth, massive MIMO has been identified as a pivotal component of future 5G systems [10]. In a cooperative relay system, when multiple relay nodes are present, relay selection can be used to increase the reliability and the data rate of a system [11]. Relay selection can be based on different performance criteria and significantly increase the performance of MIMO TWRNs [12].

In this paper we analyze relay selection problem in CR massive MIMO TWRNs with multiple relays to improve the sum rate of the system. The source and destination nodes (i.e. end nodes) are massive MIMO enabled and the relay nodes are MIMO enabled. End nodes perform zero-forcing (ZF) transmission and ZF receiving while relays perform amplify-and-forward (AF) transmission. Furthermore, the end nodes perform self-interference cancellation. The source, destination and the relay nodes all act as secondary users in the presence of a PU.

Previous Work on CR TWRNs: CR TWRNs with AF operations have been studied in [13] by obtaining detection probabilities and outage probabilities. However, this analysis is done for an overlay CR system. In [14], outage probability is analyzed for a TWRN with digital network coding and relay selection. Overlay CR systems with multiple relays have been analyzed in [15]. Furthermore, in [16], relay selection and optimal power allocation is analyzed for single antenna nodes under CR TWRN settings. In [17], CR massive MIMO systems are analyzed for power allocation under pilot contamination. Furthermore, in [18] the performance of an underlay MIMO secondary system under a MIMO primary system has been analyzed. Several results have been obtained when the number of antennas at the primary system increases to infinity. None of these work, focus on relay selection for massive MIMO CRs.

Motivation and our contribution: Significant sum rate gains and outage minimizations has been obtained through relay selection for MIMO systems [12]. Also, massive MIMO has resulted in significant power efficiencies and sum rate improvements [8]. However to the best of authors knowledge, studies on CR massive MIMO TWRNs with relay selection are not present on the current wireless research literature. This is a challenging problem because of the strict limits on PU interference. Hence, our motivation in this work is obtaining significant sum rate gains by combining relay selection, massive MIMO TWRNs, and CR. Specifically, our objective is to maximize the sum rate of a CR TWRN with multiple relays through relay selection under the peak interference constraints on the PU. We first obtain the asymptotic signal-to-interference-plus-noise ratio (SINR) and the sum rate for a certain data sub-stream, when a certain relay is selected. Then, we obtain the aggregated sum rate for the selected relay and solve the optimum power allocation to maximize the sum rate under the maximum interference constraint at PU. Finally, we present the relay selection criteria and obtain the maximum sum rate with relay selection.

Our results show that the asymptotic SINR and sum rate do not depend on the small scale fading and thus, the relay selection can be done at the designing stage of the system. If all other parameters are equal for relays, the sum rate maximization simplifies to the selection of the relay with highest number of antennas. Further, our results show that the interference on the PU can be easily reduced through the use of massive MIMO at the end nodes.

One inherent problem of a TWRN in a CR setting is the management of the interference caused on the PU. As both end nodes transmit simultaneously to the relay, the end nodes must coordinate there power levels to limit the interference on PU. This leads to complex issues such as requirement of each others channel knowledges for end nodes, which will be hard to implement in a practical application. Some previous research has solved this problem [14], [19] by using seperate time slots for end nodes. But this leads to reduced sum rates as three time slots are required for bidirectional data transfer between the end nodes. However, with the use of massive MIMO at the end nodes, we show that end nodes can transmit simultaneously without worrying about the interference on the PU.

Notation: $\mathbf{Z}^H$, $\mathbf{Z}^T$, and $[\mathbf{Z}]_{k,k}$ denote the Hermitian-transpose, transpose, and the kth diagonal element of the matrix, $\mathbf{Z}$, respectively. A complex Gaussian random variable X with mean μ and standard deviation σ is denoted as $X \sim \mathcal{CN}\left(\mu, \sigma^2\right)$.

II. System, channel, and signal model

A. System and channel model

Our system model consists of one PU and a secondary TWRN. Secondary TWRN consists of two user nodes (S_1 and S_2) and K relay nodes (R_k for $k \in \{1, \cdots, K\}$). PU is equipped with N antennas and user node S_i is equipped with N_i antennas for $i \in \{1, 2\}$, and the kth relay node has N_{R_k} antennas. All secondary nodes are assumed half-duplex terminals, and all channel amplitudes are assumed independently distributed, frequency flat-Rayleigh fading. Thus, the wireless channel from S_i to PU is defined as $\mathbf{F}_i = \tilde{\mathbf{F}}_i \hat{\mathbf{D}}_i^{1/2}$, where $\tilde{\mathbf{F}}_i \sim \mathcal{CN}_{N \times N_i}\left(\mathbf{0}_{N \times N_i}, \mathbf{I}_N \otimes \mathbf{I}_{N_i}\right)$ captures the fast fading and $\hat{\mathbf{D}}_i = \hat{\eta}_i \mathbf{I}_{N_i}$ accounts for the pathloss. The channel between R_k and PU is defined as $\mathbf{G}_k = \tilde{\mathbf{G}}_k \mathbf{D}_k^{1/2}$, with $\tilde{\mathbf{G}}_k \sim \mathcal{CN}_{N \times N_{R_k}}\left(\mathbf{0}_{N \times N_{R_k}}, \mathbf{I}_N \otimes \mathbf{I}_{N_{R_k}}\right)$ and $\mathbf{D}_k = \eta_k \mathbf{I}_{N_{R_k}}$. Similarly, the channel matrix from S_i to R_k is defined as $\mathbf{H}_{i,k} = \tilde{\mathbf{H}}_{i,k} \mathbf{D}_{i,k}^{1/2}$, with $\tilde{\mathbf{H}}_{i,k} \sim \mathcal{CN}_{N_{R_k} \times N_i}\left(\mathbf{0}_{N_{R_k} \times N_i}, \mathbf{I}_{N_{R_k}} \otimes \mathbf{I}_{N_i}\right)$ and $\mathbf{D}_{i,k} = \eta_{i,k} \mathbf{I}_{N_i}$. The detailed system model is shown in Fig. 1. The channel coefficients are assumed to be fixed during two consecutive time-slots (a time-slot is the time used for a single transmission between two wireless nodes), and hence, the reverse channels are assumed to be the transpose of forward channel by using the reciprocity property of wireless channels. The additive noise at all the receivers is modelled as complex zero mean additive white Gaussian (AWGN) noise. The direct channel between S_1 and S_2 is assumed to be unavailable due to large pathloss and heavy shadowing effects [4], [7].

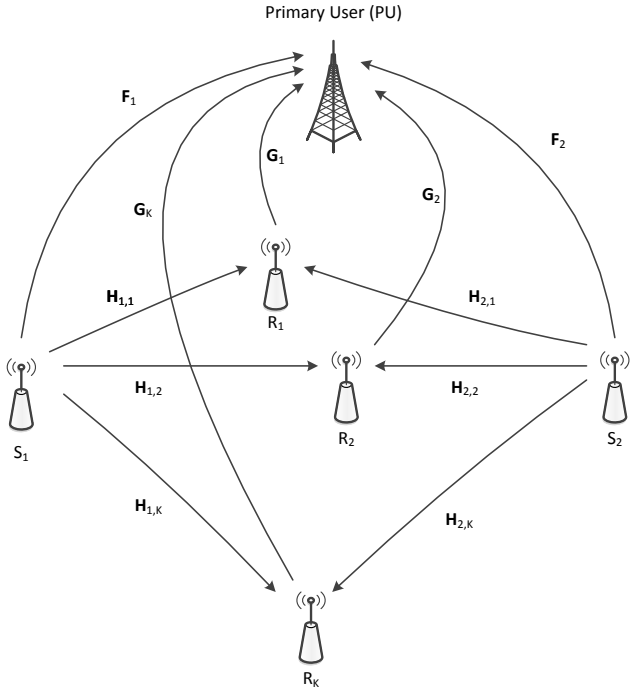

Fig. 1: The system model with K relay nodes and the channel matrices between different nodes.

B. Signal model

S_1 and S_2 exchange their signal vectors $\mathbf{x}_1$ and $\mathbf{x}_2$ by selecting one of the available relays using two time slots. Here, we denote the selected relay as R_k for the analysis. First, S_1 and S_2 transmit $\mathbf{x}_1$ and $\mathbf{x}_2$, respectively, towards R_k by employing transmit-ZF precoding over the multiple access channel[1]. The received signal at R_k can then be written as

$$\mathbf{y}_{R_k} = m_{1,k}\mathbf{H}_{1,k}\mathbf{V}_{T_{1,k}}\mathbf{x}_1 + m_{2,k}\mathbf{H}_{2,k}\mathbf{V}_{T_{2,k}}\mathbf{x}_2 + \mathbf{n}_{R_k} + \mathbf{i}_{R_k}, \quad (1)$$

where the $N_{R_k} \times 1$ signal vector $\mathbf{x}_i$ satisfies $\mathcal{E}\left[\mathbf{x}_i \mathbf{x}_i^H\right] = \mathbf{I}_{N_{R_k}}$ for $i \in \{1, 2\}$ and $k \in \{1, \cdots, K\}$. Thus, the $N_i \times 1$ precoded-transmit signal vector at S_i is given by $\mathbf{V}_{T_{i,k}}\mathbf{x}_i$. Here, $\mathbf{i}_{R_k}$ is the $N_{R_k} \times 1$ interference vector on the secondary relay by the PU, which is modelled as AWGN with average power $\sigma_{i_k}^2 = P_U \eta_k$, where P_U is the transmit power of PU.[2] In (1), $m_{i,k}$ is the power normalizing factor at S_i and is designed to constrain its transmit power as follows [7]:

$$m_{i,k} = \sqrt{\mathcal{P}_{i,k} / \mathrm{Tr}\left(\mathbf{V}_{T_{i,k}} \mathbf{V}_{T_{i,k}}^H\right)}, \quad (2)$$

where $\mathcal{P}_{i,k}$ is the transmit power at S_i to satisfy the interference constraints at PU. Further, in (1), $\mathbf{n}_{R_k}$ is the $N_{R_k} \times 1$ zero mean AWGN vector at R_k satisfying $\mathcal{E}\left(\mathbf{n}_{R_k}\mathbf{n}_{R_k}^H\right) = \mathbf{I}_{N_{R_k}}\sigma_{R_k}^2$, and $\mathbf{V}_{T_{i,k}}$ is the transmit-ZF precoding matrix at S_i given by [20]

$$\mathbf{V}_{T_{i,k}} = \mathbf{H}_{i,k}^H \left(\mathbf{H}_{i,k}\mathbf{H}_{i,k}^H\right)^{-1}. \quad (3)$$

[1]In order to use transmit-ZF at S_1 and S_2, the constraint $\min(N_1, N_2) \geq \max_{k \in \{1, \cdots, K\}} N_{R_k}$ needs to be satisfied.

[2]Here, as we assume no coordination between the primary and secondary networks, we use the average interference power at the relay when the PU is transmitting. Similar assumptions are made in [16].

$$\gamma_{S_{i,k}^{(l)}}=\frac{P_{R_k}P_{i',k}/\mathrm{Tr}\left(\left[\mathbf{H}_{i',k}\mathbf{H}_{i',k}^H\right]^{-1}\right)}{P_{R_k}\left(\sigma_{R_k}^2+\sigma_{i_k}^2\right)+\left(\frac{P_{1,k}}{\mathrm{Tr}\left(\left[\mathbf{H}_{1,k}\mathbf{H}_{1,k}^H\right]^{-1}\right)}+\frac{P_{2,k}}{\mathrm{Tr}\left(\left[\mathbf{H}_{2,k}\mathbf{H}_{2,k}^H\right]^{-1}\right)}+\sigma_{R_k}^2+\sigma_{i_k}^2\right)\frac{\sigma_{N_i}^2+\sigma_{I_i}^2}{\eta_{i,k}}\left[\left(\tilde{\mathbf{H}}_{k,i}^H\tilde{\mathbf{H}}_{k,i}\right)^{-1}\right]_{l,l}}, \tag{14}$$

In the second time-slot, R_k amplifies $\mathbf{y}_{R_k}$ and broadcasts this amplified-signal towards both user nodes. Each node then performs ZF receiving and obtains the following signal vector:

$$\mathbf{y}_{S_{i,k}}=\mathbf{V}_{R_{i,k}}\left(M_k\mathbf{H}_{k,i}\mathbf{y}_{R_k}+\mathbf{n}_i+\mathbf{i}_i\right), \tag{4}$$

where M_k is the amplification factor at R_k and is defined as

$$M_k=\sqrt{\mathcal{P}_{R_k}/\left(m_{1,k}^2+m_{2,k}^2+\sigma_{R_k}^2+\sigma_{i_k}^2\right)}, \tag{5}$$

where $m_{k,i}$ is defined in (2) and $\mathcal{P}_{R_k}$ is the transmit power at R_k to satisfy the interference constraints at PU. Moreover, in (4), $\mathbf{H}_{k,i}=\mathbf{H}_{i,k}^T$, and $\mathbf{n}_i$ is the $N_i\times 1$ zero mean AWGN at S_i satisfying $\mathcal{E}\left(\mathbf{n}_i\mathbf{n}_i^H\right)=\mathbf{I}_{N_i}\sigma_i^2$. Also, $\mathbf{i}_i$ is the interference on S_i by PU with average power $\sigma_i^2=P_U\hat{\eta}_i$. Besides, $\mathbf{V}_{R_{i,k}}$ is the receive-ZF matrix at S_i and can be written as [20]

$$\mathbf{V}_{R_{i,k}}=\left(\mathbf{H}_{k,i}^H\mathbf{H}_{k,i}\right)^{-1}\mathbf{H}_{k,i}^H. \tag{6}$$

C. Effect on the Primary User

In underlay cognitive radio, the secondary users should transmit their data without exceeding the interference temperature at the PU. Thus, in this section we obtain the equations for the received interference at the PU during the two time slots. During the first time-slot, the received interference signal at PU can then be written as

$$\mathbf{i}_{1,k}=m_{1,k}\mathbf{F}_1\mathbf{V}_{T_{1,k}}\mathbf{x}_1+m_{2,k}\mathbf{F}_2\mathbf{V}_{T_{2,k}}\mathbf{x}_2. \tag{7}$$

Similarly, in the second time-slot, the received interference signal at PU can then be written as

$$\begin{aligned}\mathbf{i}_{2,k}&=M_k\mathbf{G}_k y_{R_k}\\&=m_{1,k}M_k\mathbf{G}_k\mathbf{H}_{1,k}\mathbf{V}_{T_{1,k}}\mathbf{x}_1+m_{2,k}M_k\mathbf{G}_k\mathbf{H}_{2,k}\mathbf{V}_{T_{2,k}}\mathbf{x}_2\\&+M_k\mathbf{G}_k\mathbf{n}_{R_k}+M_k\mathbf{G}_k\mathbf{i}_{R_k}.\end{aligned} \tag{8}$$

The received interference powers for the above two cases and the interference constraint at the PU is given as

$$I_{1,k}=P_{1,k}\mathrm{Tr}\left(\mathbf{F}_1^H\mathbf{F}_1\right)+P_{2,k}\mathrm{Tr}\left(\mathbf{F}_2^H\mathbf{F}_2\right)\le I_t, \tag{9}$$

$$I_{2,k}=P_{R_k}\mathrm{Tr}\left(\mathbf{G}_k^H\mathbf{G}_k\right)\le I_t, \tag{10}$$

where I_t is the acceptable interference level at PU.

D. Exact conditional end-to-end SINR

In this subsection, we obtain the exact end-to-end SINR of the lth data substream for $l\in\{1,\cdots,N_{R_k}\}$ under the transmit powers of $P_{1,k},P_{2,k}$ and P_{R_k}. To this end, by substituting (1), (3), and (6) into (4), the received signal vector at S_i can be written in an alternative form as follows:

$$\mathbf{y}_{S_{i,k}}=M_k\left(m_{i,k}\mathbf{x}_i+m_{i',k}\mathbf{x}_{i'}+\mathbf{n}_{R_k}+\mathbf{i}_{R_k}\right)+\tilde{\mathbf{n}}_i, \tag{11}$$

where $\{i,i'\}\in\{\{1,2\},\{2,1\}\}$. Further, $\tilde{\mathbf{n}}_i$ is the filtered, colored noise and is given by $\tilde{\mathbf{n}}_i=\mathbf{V}_{R_{i,k}}\left(\mathbf{n}_i+\mathbf{i}_i\right)$. Next, by using self-interference cancellation to (11), the signal vector of $S_{i'}$ received at S_i can be extracted as follows:

$$\tilde{\mathbf{y}}_{S_{i,k}}=M_k\left(m_{i',k}\mathbf{x}_{i'}+\mathbf{n}_{R_k}+\mathbf{i}_{R_k}\right)+\tilde{\mathbf{n}}_i. \tag{12}$$

By using (12), the post-processing end-to-end SINR of the lth data substream at S_i can be derived as

$$\gamma_{S_{i,k}^{(l)}}=\frac{M_k^2m_{i',k}^2}{M_k^2\sigma_{R_k}^2+M_k^2\sigma_{i_k}^2+\frac{\sigma_{N_i}^2+\sigma_{I_i}^2}{\eta_{i,k}}\left[\left(\tilde{\mathbf{H}}_{k,i}^H\tilde{\mathbf{H}}_{k,i}\right)^{-1}\right]_{l,l}}, \tag{13}$$

where $\{i,i'\}\in\{\{1,2\},\{2,1\}\}$, $l\in\{1,\cdots,N_{R_k}\}$, and $k\in\{1,\cdots,K\}$. By substituting M_k (5), $m_{i',k}$ (2) and the result $\mathrm{Tr}\left(\mathbf{V}_{T_{i,k}}\mathbf{V}_{T_{i,k}}^H\right)=\mathrm{Tr}\left(\left[\mathbf{H}_{i,k}\mathbf{H}_{i,k}^H\right]^{-1}\right)$ into (13), the end-to-end conditional SINR in (13) can be written in a more insightful form as (14) at the top of this page.

E. Sum rate analysis when R_k is selected

In this subsection, we obtain sum rate expressions when the relay R_k is selected assuming that the interference constraints at PU is satisfied. To correctly decode the data substreams by the receivers, each node need to transmit the data in common rate in MIMO TWRNs. Thus, the sum rate obtained by selecting kth relay can be defined as follows:

$$\mathcal{R}_k=2\min\left(\mathcal{R}_{S_{1,k}},\mathcal{R}_{S_{2,k}}\right), \tag{15}$$

where $\mathcal{R}_{S_{i,k}}$ is the sum of data substreams rates at S_i for $i\in\{1,2\}$, and can be written as

$$\mathcal{R}_{S_{i,k}}=\frac{1}{2}\sum_{l=1}^{N_{R_k}}\log\left(1+\gamma_{S_{i,k}^{(l)}}\right). \tag{16}$$

The factor of two appears in (15) due to the presence of two user nodes in the TWRN of interest. Further, the pre-log factor of one-half in (16) is due to the use of two time-slots.

III. Asymptotic Analysis

In this section we analysis the interference conditions and conditional end-to-end SINR under the asymptotic limits (i.e. $N_1,N_2\to\infty$) and with power scaling at the relay and end nodes. While the number of antennas at the user nodes S_1 and S_2, N_1 and N_2 grows unbounded, the number of antennas at the relay node R_k and PU is kept unchanged. For simplicity it is assumed that as $N_1,N_2\to\infty$, the ratio between the number of antennas at S_1 and S_2 is kept constant for analytical simplicity. Thus

$$\alpha=\frac{N_2}{N_1}. \tag{17}$$

As the number of antennas at the user nodes asymptotically approaches ∞, we use the following identity from [8] as

$$\gamma_{S_{1,k}^{(l)}}^{\infty} = \frac{E_{R_k} E_{2,k} \eta_{1,k} \eta_{2,k}}{\left(\sigma_{N_i}^2 + \sigma_{I_i}^2\right)\left(E_{1,k}\eta_{1,k} + E_{2,k}\eta_{2,k}\right) + \left(\sigma_{R_k}^2 + \sigma_{i_k}^2\right) N_{R_k}\left(E_{R_k}\eta_{1,k} + \sigma_{N_i}^2 + \sigma_{I_i}^2\right)}, \tag{23}$$

$$\gamma_{S_{2,k}^{(l)}}^{\infty} = \frac{\alpha E_{R_k} E_{1,k} \eta_{1,k} \eta_{2,k}}{\left(\sigma_{N_i}^2 + \sigma_{I_i}^2\right)\left(E_{1,k}\eta_{1,k} + E_{2,k}\eta_{2,k}\right) + \left(\sigma_{R_k}^2 + \sigma_{i_k}^2\right) N_{R_k}\left(\alpha E_{R_k}\eta_{2,k} + \sigma_{N_i}^2 + \sigma_{I_i}^2\right)}, \tag{24}$$

$$\lim_{N_i \to \infty} \frac{\mathbf{H}_{i,k}\mathbf{H}_{i,k}^H}{N_i} = \mathbf{D}_{i,k}. \tag{18}$$

The transmit power at the user nodes S_1 and S_2 and the transmit power at the relay nodes R_k for $k \in \{1, \cdots, K\}$ are scaled inversely proportional to the number of antennas at the user nodes. Thus

$$P_{i,k} = \frac{E_{i,k}}{N_1} \quad \text{for} \quad i \in \{1,2\} \quad \text{and} \quad P_{R_k} = \frac{E_{R_k}}{N_1}, \tag{19}$$

where $E_{1,k}$, $E_{2,k}$ and E_{R_k} are fixed. By substituting these values we rewrite (10) as

$$I_{2,k} = E_{R_k} \frac{\text{Tr}\left(\mathbf{G}_k^H \mathbf{G}_k\right)}{N_1} \leq I_t, \tag{20}$$

and as $\frac{\text{Tr}\left(\mathbf{G}_k^H \mathbf{G}_k\right)}{N_1} \to 0$ as $N_1 \to \infty$, this condition is asymptotically satisfied for any value of E_{R_k}. By using

$$\lim_{N_i \to \infty} \frac{\text{Tr}\left(\mathbf{F}_i^H \mathbf{F}_i\right)}{N_i} = \hat{\eta}_i N, \tag{21}$$

on eqn. (9) we obtain the interference constraint as

$$\lim_{N_i \to \infty} I_{1,k} = E_{1,k}\hat{\eta}_1 N + E_{2,k}\hat{\eta}_2 N \leq I_t, \tag{22}$$

By using the asymptotic limit results on (14), we obtain the asymptotic SINRs for this case as (23) and (24) at the top of this page when condition (22) is satisfied. Here, $k \in \{1, \cdots, K\}$ and $l \in \{1, \cdots, N_{R_k}\}$. Interestingly, the asymptotic SINRs in (23) and (24), are independent of the fast fading component of the wireless channel, and only depend on pathloss of the channels. It is worth noting that the asymptotic SINRs are independent of the data-stream index, k, as well, and hence, we can denote $\gamma_{S_{i,k}^{(l)}}^{\infty} = \gamma_{S_{i,k}}^{\infty}$ for $l \in \{1, \cdots, N_{R_k}\}$. By substituting this value in (16) we obtain the sum rate between U_i and R_k as

$$\mathcal{R}_{S_{i,k}}^{\infty} = \frac{1}{2} N_{R_k} \log\left(1 + \gamma_{S_{i,k}}^{\infty}\right). \tag{25}$$

Further, we obtain the total sum rate when R_k is selected as

$$\mathcal{R}_k^{\infty} = N_{R_k} \log\left(1 + \min\left(\gamma_{S_{1,k}}^{\infty}, \gamma_{S_{2,k}}^{\infty}\right)\right), \tag{26}$$

Remark I: As mentioned earlier, the results obtained in (23) and (24), only depend on the pathloss coefficient and the average noise values. Thus, the sum rate of the system will be a fixed value for a specified relay. Thus, relay selection can be done at the designing stage and no instantaneous channel information will be required for the relay selection process.

IV. Optimal power allocation and relay selection

A. Optimal power allocation

In this section we obtain the optimal power allocation results to maximize the sum rate given in (26) under the interference constraint in (22). We represent the optimal power allocation at S_1 and S_2 as $E_{1,k}^*$ and $E_{2,k}^*$. First, we analyze the sum rate maximization through power allocation for the data transmission through relay node R_k.

Maximizing R_k^{∞} corresponds to deciding power allocation to $E_{1,k}$ and $E_{2,k}$ to maximizing the minimum of $\gamma_{S_{1,k}}^{\infty}$ and $\gamma_{S_{2,k}}^{\infty}$. By observing that both (23) and (24) are increasing with respect to $E_{1,k}$ and $E_{2,k}$, we can deduce that the maximum value occurs when $\gamma_{S_{1,k}}^{\infty} = \gamma_{S_{2,k}}^{\infty}$. By substituting

$$E_{1,k}^* = \frac{1}{\hat{\eta}_1}\left(\frac{(1+\delta)}{N} I_t - E_{2,k}^* \hat{\eta}_2\right), \tag{27}$$

to (23) and (24), and by using the equality, we can obtain a quadratic equation to solve $E_{1,k}^*$ and $E_{2,k}^*$. Here, $0 \leq \delta \ll 1$ and is used to make sure that the interference on PU is significantly less than the threshold. We denote the asymptotic SINR values and the sum rate value corresponding to this optimum allocation case as $\gamma_{S_{1,k}}^{\infty,*}$, $\gamma_{S_{1,k}}^{\infty,*}$, and $\mathcal{R}_k^{\infty,*}$ respectively.

As an special case, if we assume that $\alpha = 1$ and $\eta_{1,k} = \eta_{2,k}$, then we can conclude that $E_{1,k}^* = E_{2,k}^*$. By using (27) we obtain

$$E_{1,k}^* = E_{2,k}^* = \frac{1+\delta}{\left(\hat{\eta}_1 + \hat{\eta}_2\right) N} I_t. \tag{28}$$

B. Relay selection with optimum values

In this section we obtain the asymptotic sum rate with optimal power allocation and relay selection. The optimum relay selection criteria to maximize the sum rate of the secondary system can be given as

$$\begin{aligned} K^* &= \underset{k \in \{1, \cdots, K\}}{\text{argmax}} \left[\mathcal{R}_k^{\infty,*}\right] \\ &= \underset{k \in \{1, \cdots, K\}}{\text{argmax}} \left[N_{R_k} \log\left(1 + \min\left(\gamma_{S_{1,k}}^{\infty}, \gamma_{S_{2,k}}^{\infty}\right)\right)\right], \end{aligned} \tag{29}$$

where K^* is the selected relay index. Further, (29) shows that the optimal relay selection highly depends on the maximum value of N_{R_k}. Since, N_{R_k} appears outside of the logarithm, the impact of N_{R_k} is higher. Thus, for most cases the relay selection will be simplified to selection of the relay with the maximum number of antennas. Thus, we propose selection of the relay with the maximum number of antennas to maximize the sum rate of the system.

Remark II: This result shows that, if the number of antennas of each relay and other parameters are the same, then the relay selection does not increase the asymptotic sum rate. Thus, in such a scenario, just selecting a random relay will still give maximum asymptotic sum rate without the overhead costs of relay selection.

V. Numerical Results

In this section, our numerical and simulation results are presented to study the performance of our proposed selection strategy by plotting the average sum rate and asymptotic sum rate. We use

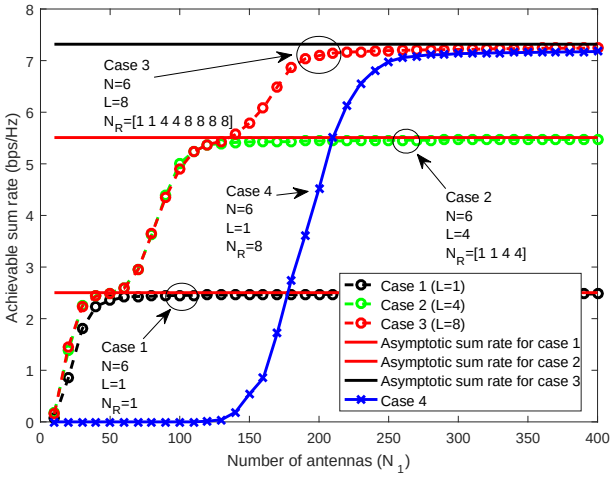

Fig. 2: The sum rate comparisons for different number of relays L vs the number of antennas at the S_1 nodes. Different relays have different number of antennas.

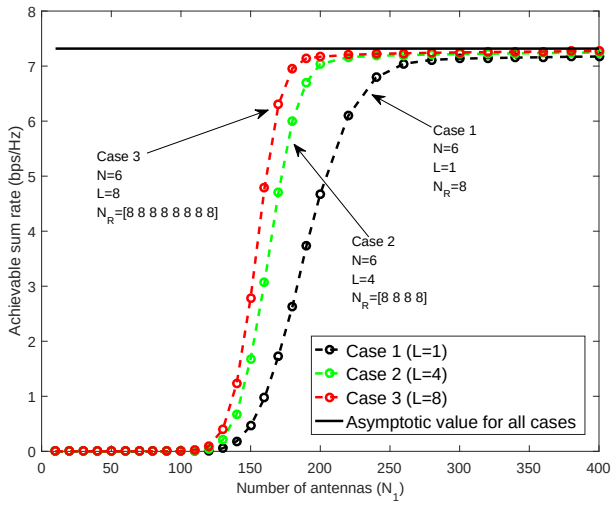

Fig. 3: The sum rate comparisons for different number of relays K vs the number of antennas at the S_1 nodes. All relays have 8 antennas.

interference threshold at PU as $I_T = 10$dB, the large scale fading coefficients between PU and S_1 and S_2 as $\hat{\eta}_1 = \hat{\eta}_2 = 1/16$, and the noise powers $\sigma^2_{N_i} = \sigma^2_{R_k} = 1$. We also set $\alpha = 1$ and transmit power at the relay R_k as $E_k = 25$dB. The primary user has 6 antennas (i.e. $N = 6$). In Fig. 2, we analyze our results for four cases with different number of relays. Case one consists of a single relay node (i.e. $K = 1$) with a single antenna. In case two, $K = 4$ and the number of antennas at the relays (N_k) are $1, 1, 4, 4$ respectively. In case three, we have $K = 8$ and the number of antennas at the relays are $1, 1, 4, 4, 8, 8, 8, 8$ respectively. In fourth case, we plotted the sum rate, when the relay with highest number fo antennas is selected (i.e. relay with 8 antennas). We have used the optimal power allocation scheme we derived with $\delta = 0.1$. It can be seen from this figure that significant sum rate gains can be obtained through having multiple relays. As an example a single relay with a single antenna can only achievable a sum rate of 2.5bps/Hz while the four-relay system which has $1, 1, 4$, and 4 antennas each can obtain a achievable sum rate of 5.5bps/Hz. Also, with eight relays, the achievable sum rate is 7.2bps/Hz which offers a significant increase compared to previous two cases. Our asymptotic analysis perfectly matches the simulated sum rates when the number of antennas are increased. Selecting the relay with the highest number of antennas (case 4) provides the same asymptotic sum rate as case 3 which uses relay selection. However, without relay selection, higher number of antennas are required to achieve asymptotic performance. In Fig. 3, we analyze the sum rate of the system with different number of relays, but when those relays have the same number of antennas (i.e. $N_k = 8$ for all the relays). Case one, two, and three corresponds to 1, 4, and 8 relays respectively. Optimal power allocation with $\delta = 0.1$ is used. Unlike in Fig. 2, we can see that the achievable asymptotic sum rates for different cases are the same. This is due to the fact that the achievable sum rate depends on the relay with the highest number of antennas. However, with multiple relays, the asymptotic performance can

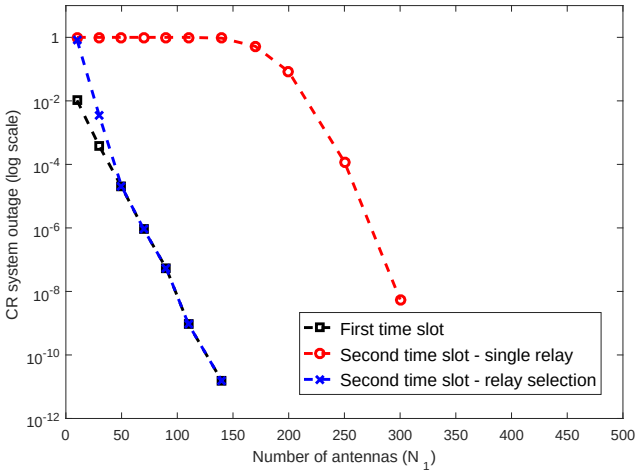

Fig. 4: The outage of the CR TWRN during different time slots with and without relay selection.

be obtained by using a smaller number of antennas at the end nodes. Also it can be seen that until the number of antennas at the end nodes surpasses a certain number (in this case around 120), the achievable sum rate of the system is zero. This is due to the interference constraint at the PU. Although eqn. (9) is satisfied asymptotically for any E_{R_k}, when N_1 is low this constraint may not be satisfied and the secondary system will remain in outage state. Thus, until the number of antennas at the end nodes increases upto a certain limit, the secondary network cannot start the transmission.

In Fig. 4, we have plotted the probability of outage of the system due to the interference at the PU exceeding the threshold level. We have plotted (1) interference during the first time slot (i.e. when both the end nodes are transmitting) causes the outage, (2) interference during the second time slot causes the outage when having 8 antennas, and (3) interference during the second

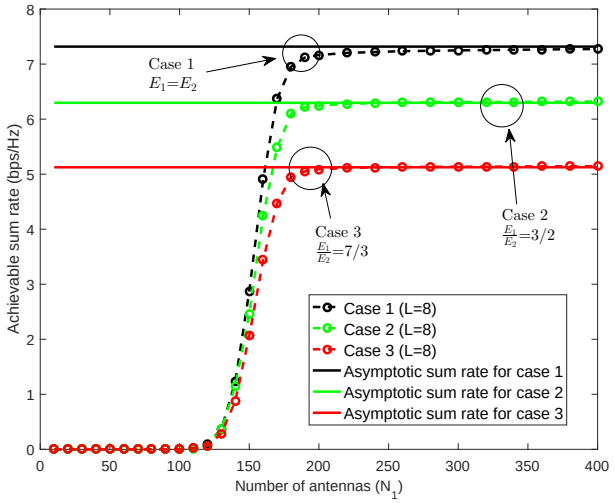

Fig. 5: The achievable sum rate of the system against the number of antennas at the end nodes for different power allocation cases.

time slot causes the outage when the relay with the highest number of antennas is selected. As seen from the Fig. 4, the outage probability of the system due to interference on first time slot rapidly reduces with the number of antennas. As an example, with 200 antennas the outage is less than 10^{-12}. This shows that, with a large antenna array at the end nodes and power scaling, the interference at the PU approaches 0 and thus, the end nodes does not need to know each others channel matrices to decide whether to transmit or not. Also, the interference during the second time slot approaches zero but with a less convergence rate. As an example with 250 antennas, relay selection provides less than 10^{-12} outage while the outage with a single relay is around 10^{-5}. In Fig. 5, we plot the achievable sum rates for three cases for different power allocations at the end nodes. In case one, we use the optimal power allocation scheme we derived. In case 2, we use $\frac{E1}{E_2} = 3/2$ and in case 3, we use $\frac{E_1}{E_2} = 7/3$. it can be seen from the plot that the sum rate approaches the asymptotic sum rates we obtained through equations when the number of antennas at the end nodes increases. Furthermore, our optimal power allocation scheme obtains the highest achievable sum rate while the sum rates of other power allocations are significantly less than the sum rate we obtained for the optimal power allocation.

VI. Conclusion

In this paper, we analyzed a massive MIMO CR TWRN with relay selections to maximize the sum rate. With the use of massive MIMO at the secondary end nodes, the asymptotic SINR becomes independent of small scale fading and only depends on the number of antennas at the relay, pathloss coefficients between nodes, the average noise and interference powers, and the transmit powers at end nodes. Furthermore, we obtained the optimal power allocation at end nodes under the interference limited constraint at PU. Use of massive MIMO at the end nodes of a CR TWRN increases the achievable sum rate of the secondary network and decreases the interference on the PU. Most of the time, relay selection for a CR TWRN with massive MIMO end nodes simplifies to the selection of the relay with the highest number of antennas. However, if all the relays have the same number of antennas, relay selection does not increase the asymptotic performance.

References

[1] (2016) Cisco visual networking index: Global mobile data traffic forecast update, 2015-2020. CISCO. [Online]. Available: http://www.cisco.com/c/en/us/solutions/collateral/service-provider/visual-networking-index-vni/mobile-white-paper-c11-520862.pdf

[2] S. Haykin, "Cognitive radio: brain-empowered wireless communications," *IEEE J. Sel. Areas Commun.*, vol. 23, no. 2, pp. 201–220, Feb. 2005.

[3] A. Goldsmith, S. A. Jafar, I. Maric, and S. Srinivasa, "Breaking spectrum gridlock with cognitive radios: An information theoretic perspective," *Proc. IEEE*, vol. 97, no. 5, pp. 894–914, May 2009.

[4] B. Rankov and A. Wittneben, "Spectral efficient protocols for half-duplex fading relay channels," *IEEE J. Sel. Areas Commun.*, vol. 25, no. 2, pp. 379–389, Feb. 2007.

[5] K. Loa, C.-C. Wu, S.-T. Sheu, Y. Yuan, M. Chion, D. Huo, and L. Xu, "IMT-advanced relay standards," *IEEE Commun. Mag.*, vol. 48, no. 8, pp. 40–48, Aug. 2010.

[6] A. Paulraj, R. Nabar, and D. Gore, *Introduction to space-time wireless communications*, 1st ed. Cambridge, UK ; New York, NY : Cambridge University Press, 2003.

[7] G. Amarasuriya, C. Tellambura, and M. Ardakani, "Performance analysis of zero-forcing for two-way MIMO AF relay networks," *IEEE Wireless Commun. Lett.*, vol. 1, no. 2, pp. 53–56, Apr. 2012.

[8] T. L. Marzetta, "Noncooperative cellular wireless with unlimited numbers of base station antennas," *IEEE Trans. Wireless Commun.*, vol. 9, no. 11, pp. 3590–3600, Nov. 2010.

[9] F. Rusek, D. Persson, B. K. Lau, E. Larsson, T. Marzetta, O. Edfors, and F. Tufvesson, "Scaling up MIMO: Opportunities and challenges with very large arrays," *IEEE Signal Process. Mag.*, vol. 30, no. 1, pp. 40–60, Jan. 2013.

[10] J. Andrews, S. Buzzi, W. Choi, S. Hanly, A. Lozano, A. Soong, and J. Zhang, "What will 5G be?" *IEEE J. Sel. Areas Commun.*, vol. 32, no. 6, pp. 1065–1082, Jun. 2014.

[11] A. Bletsas, A. Khisti, D. P. Reed, and A. Lippman, "A simple cooperative diversity method based on network path selection," *IEEE J. Sel. Areas Commun.*, vol. 24, no. 3, pp. 659–672, Mar. 2006.

[12] S. Silva, G. Amarasuriya, C. Tellambura, and M. Ardakani, "Relay selection strategies for MIMO two-way relay networks with spatial multiplexing," *IEEE Trans. Commun.*, vol. 63, no. 12, pp. 4694–4710, Dec. 2015.

[13] G. Wang, Y. Zou, J. Lu, and C. Tellambura, "Cognitive transmission and performance analysis for amplify-and-forward two-way relay networks," in *2014 IEEE International Conference on Communications (ICC)*, Jun. 2014, pp. 5843–5848.

[14] T. T. Duy and H. Y. Kong, "Exact outage probability of cognitive two-way relaying scheme with opportunistic relay selection under interference constraint," *IET Communications*, vol. 6, no. 16, pp. 2750–2759, Nov. 2012.

[15] Y. Zou, Y. D. Yao, and B. Zheng, "Cognitive transmissions with multiple relays in cognitive radio networks," *IEEE Trans. Commun.*, vol. 10, no. 2, pp. 648–659, Feb. 2011.

[16] P. Ubaidulla and S. Aissa, "Optimal relay selection and power allocation for cognitive two-way relaying networks," *IEEE Wireless Commun. Lett.*, vol. 1, no. 3, pp. 225–228, Jun. 2012.

[17] S. Kusaladharma and C. Tellambura, "Massive MIMO based underlay networks with power control," in *2016 IEEE International Conference on Communications (ICC)*, May 2016, pp. 1–6.

[18] L. Wang, H. Q. Ngo, M. Elkashlan, T. Q. Duong, and K. K. Wong, "Massive MIMO in spectrum sharing networks: Achievable rate and power efficiency," *IEEE Systems Journal*, vol. PP, no. 99, pp. 1–12, 2015.

[19] K. B. Fredj and S. Aissa, "Performance of spectrum-sharing constrained two-way relaying," in *2014 IEEE Wireless Communications and Networking Conference (WCNC)*, April 2014, pp. 845–850.

[20] R. W. Heath, S. Sandhu, and A. Paulraj, "Antenna selection for spatial multiplexing systems with linear receivers," *IEEE Commun. Lett.*, vol. 5, no. 4, pp. 142–144, Apr. 2001.